AEM Accepts, published online ahead of print on 17 October 2014
Appl. Environ. Microbiol. doi:10.1128/AEM.02920-14

Enhancing terpene yield from sugars via novel routes to 1-deoxy-D-xylulose 5-phosphate.

James Kirby,[a,b] Minobu Nishimoto,[a,b] Ruthie W.N. Chow,[a] Edward E. K. Baidoo,[b] George Wang,[b] Joel Martin,[e] Wendy Schackwitz,[e] Rossana Chan,[a] Jeffrey L. Fortman,[a] and Jay D. Keasling[a,b,c,d,#]

California Institute of Quantitative Biosciences (QB3), University of California, Berkeley, California, USA[a]; Joint BioEnergy Institute, Emeryville, California, USA[b]; Department of Chemical & Biomolecular Engineering, University of California, Berkeley, California, USA[c]; Physical Biosciences Division, Lawrence Berkeley National Laboratory, Berkeley, California, USA[d]; Joint Genome Institute, Walnut Creek, California, USA[e]

Running title: novel routes to DXP

Address correspondence to: Jay D. Keasling, keasling@berkeley.edu

Journal section: Biotechnology

ABSTRACT

Terpene synthesis in the majority of bacterial species, together with plant plastids, takes place via the 1-deoxy-D-xylulose 5-phosphate (DXP) pathway. The first step of this pathway involves the condensation of pyruvate and glyceraldehyde 3-phosphate by DXP synthase (Dxs), with one sixth of the carbon lost as CO_2. A hypothetical route (nDXP) from a pentose phosphate to DXP could enable a more direct pathway from C5 sugars to terpenes and also circumvent regulatory mechanisms that control Dxs, but there is no enzyme known that can convert a sugar into its 1-deoxy equivalent. Employing a selection for complementation of a *dxs* deletion in *E. coli* grown on xylose as sole carbon source, we uncovered two candidate nDXP genes. Complementation was achieved via either overexpression of the wild type *E. coli yajO* gene, annotated as a putative xylose reductase, or via various mutations in the native *ribB* gene. In vitro analysis with purified YajO and mutant RibB proteins revealed that in both cases DXP was synthesized from ribulose 5-phosphate (Ru5P). We demonstrate utility of these genes for microbial terpene biosynthesis by engineering the DXP pathway in *E. coli* for production of the sesquiterpene bisabolene, a candidate biodiesel. To further improve flux into the pathway from Ru5P, nDXP enzymes were expressed as fusions to DXP reductase, Dxr, the second enzyme in the DXP pathway. Expression of a Dxr-RibB(G108S) fusion improved bisabolene titers more than 4-fold and alleviated accumulation of intracellular DXP.

INTRODUCTION

Terpenes constitute a considerably large family of natural products, members of which are produced in virtually all free-living organisms (1). The diverse array of structures within the terpene family is reflected by the variety of applications in society, ranging from nutrition

(carotenoids) and medicine (artemisinin, Taxol) to industrial materials (isoprene, linalool) and candidate biofuels (farnesane, bisabolane, pinene) (2). Terpenes can be synthesized via either the mevalonate or 1-deoxy-D-xylulose 5-phosphate (DXP) pathway, the former predominating in the eukaryotic cytosol and the latter in plastids, while prokaryotes may contain either pathway or in some cases both together (3).

Commercial-scale terpene production has been demonstrated in a variety of organisms, for example carotenoids via the DXP pathway in algae (4, 5), Taxol via DXP in *Taxus sp.*(6), and artemisinin via mevalonate in *Saccharomyces cerevisiae* (7). Key metrics in determining the likelihood of commercial viability are yield, productivity, and titer, particularly when targeting terpenes valued within the range of commodity chemicals or biofuels (8, 9). Of the two metabolic routes, the DXP pathway is considered the better option from a pathway efficiency viewpoint—for example the theoretical maximum yield of isoprene from glucose is around 20% higher if synthesized via DXP instead of mevalonate (9, 10). When considering production of terpenes from hemicellulosic feedstocks, conversion efficiencies of pentoses, predominantly xylose and arabinose, should also be taken into account (11). Although DXP is structurally similar to pentose phosphates, it is synthesized by DXP synthase (Dxs) via condensation of pyruvate and glyceraldehyde 3-phosphate, with a concomitant loss of CO_2. Dxs is a key control point in the pathway, and has been found to be regulated at the transcriptional and translational level as well as being feedback inhibited by the prenyl phosphates (12). We reasoned that a novel route from a pentose phosphate to DXP (nDXP) could have several advantages from a pathway engineering standpoint, including carbon-conservation, avoidance of regulatory mechanisms that target Dxs, and a more direct entry point for pentoses into the terpene biosynthetic pathway.

However, to our knowledge there are no 1-deoxy sugars made from sugars in nature, and we therefore decided to employ a directed evolution strategy.

We report the discovery of two nDXP routes following complementation of a *dxs* deletion in *E. coli* grown on xylose. One of these arose through spontaneous mutations in the native *ribB* coding sequence (cds), normally involved in riboflavin biosynthesis (13). The second route was discovered following overexpression of one of several rationally selected candidate nDXP genes, *yajO*, located next to *dxs* on the *E. coli* chromosome and annotated as a putative xylose reductase, although little evidence has been found to support this proposed function (14). Both nDXP enzymes were found to catalyze conversion of ribulose 5-phosphate (Ru5P) to DXP, providing a direct route from pentoses to terpenes (Fig. 1).

In order to test the utility of the nDXP genes for terpene production in *E. coli* we engineered a strain for production of the sesquiterpene bisabolene, a biofuel candidate, by overexpression of pathway enzymes previously found to be limiting. Coexpression of the nDXP genes enhanced bisabolene production 2-3 fold, while translational fusions to the succeeding pathway enzyme, DXP reductase (Dxr), increased production up to 4.3-fold.

MATERIALS AND METHODS

Generation of an *E. coli dxs* knockout. To permit deletion of *dxs*, *E. coli* MG1655 was first transformed with the plasmid pMBI (15), harboring four genes (*ERG12*, mevalonate kinase, *ERG8*, phosphomevaloante kinase, and *MVD1*, mevalonate pyrophosphate decarboxylase, all from *Saccharomyces cerevisiae*; and *idi*, IPP isomerase from *E. coli*), that enable biosynthesis of the isoprenoid precursors IPP and DMAPP when mevalonate is supplied exogenously to cells. Following transformation with pMBI, λ Red recombinase was used to replace the *dxs* cds with a

kanamycin marker cassette (16), generating the strain Δ*dxs*MB (Table 1). After selection on kanamycin, deletion of *dxs* was confirmed by several diagnostic PCRs, together with verification of mevalonate auxotrophy.

Use of selective pressure to isolate spontaneous nDXP mutants. Subculturing of Δ*dxs*MB was carried out in EZ Rich medium (Teknova, Hollister, CA, USA) containing 1% D-xylose (Sigma-Aldrich) as carbon source (EZ-X). Selective pressure was applied by reducing the concentration of mevalonate (Sigma-Aldrich) from 1.0 mM to 0.1 mM over the course of three cultures (subcultured at mid-log phase, 1/1000 dilution), and thereafter maintaining mevalonate at 0.1 mM. At each subculture, aliquots containing approximately 10^9 cells were plated onto EZ-X agar lacking mevalonate. Colonies were initially ranked in order of size and further prioritized based on growth in liquid medium lacking mevalonate and containing either glucose or xylose.

Genome sequencing of mevalonate-independent Δ*dxs*MB strains. Strains isolated under selective pressure that grew well in the absence of mevalonate were submitted to the Joint Genome Institute (JGI) for genome sequencing, using the parent Δ*dxs*MB strain as a reference. Libraries were generated from 1 µg of genomic DNA using a modified version of Illumina's standard protocol (Illumina Inc., Hayward, CA, USA). DNA was sheared using a sonicator (Covaris, Inc., Wolburn, MA, USA) to generate fragments of 200-800 bp in length and the fragments were then size selected by solid phase reversible immobilization (SPRI) to around 300 bp (Beckman Coulter, Indianapolis, IN, USA). Selected fragments were end-repaired, phosphorylated, and A-tailed using the polymerase activity of the Klenow fragment of E. coli DNA polymerase I, and then ligated with Illumina paired-end sequencing adapters and amplified by 10 cycles of PCR. The prepared sample libraries were quantified using the KAPA next-generation sequencing library qPCR kit (KAPA Biosystems, Wolburn, MA, USA) and run on a

LightCycler 480 real-time PCR instrument (Roche, Pleasonton, CA, USA). The quantified sample libraries were then prepared for sequencing on the Illumina sequencing platform utilizing a paired-end cluster generation kit, v4, and Illumina's cBot instrument to generate clustered flowcells for sequencing. Sequencing of the flowcells was performed on the Illumina GAIIx sequencer using SBS sequencing kits, v4, following a 2x36 run recipe.

Generation of additional ribB mutants. To screen for additional *ribB* mutations that complement Δ*dxs*, two approaches were taken, chemical mutagenesis by hydroxylamine (Sigma-Aldrich) and error-prone PCR (EP-PCR) mutagenesis. Hydroxylamine mutagenesis was performed as described previously (17) except that DNA was cleaned up using a QIAquick PCR Purification Kit (Qiagen, Valencia, CA, USA). EP-PCR mutagenesis was performed using the Clontech Diversify approach (Clontech, Mountain View, CA, USA) using conditions 2 and 5 in the manufacturer's protocol, predicted to generate 2.3 and 4.6 mutations per kb, respectively. The *ribB* cds was cloned between the NcoI and HindIII sites of pTrc99A, under control of the isopropyl-β-D-thiogalactopyranoside (IPTG) inducible trc promoter (Table 1). Mutant libraries were transformed into Δ*dxs*MB and grown under selective pressure as described above except that 50 µM IPTG (Calbiochem, EMD Millipore, Billerica, MA, USA) was included in media to induce *ribB* expression. Plasmids were recovered from mevalonate-independent strains, which were isolated from EZ-X agar plates and ranked in order of growth, and the *ribB* cds was sequenced.

Expression of other candidate nDXP genes. Several genes or gene combinations were investigated for their ability to complement a *dxs* knockout and overexpression of one of these candidates, *yajO* from *E. coli*, enabled mevalonate-independent growth. The *yajO* cds was cloned between the NcoI and HindIII sites of pTrc99A (Table 1), transformed into Δ*dxs*MB, and

then grown under selective pressure in the presence of 50 µM IPTG. EP-PCR mutagenesis of *yajO* was carried out as described for *ribB* above.

In vitro analysis of RibB(G108S) and YajO. Coding sequences for RibB(G108S) and YajO were amplified by PCR using reverse primers that added sequence encoding C-terminal StrepII peptide tags (WSHPQFEK), and cloned into pTrc99A (Table 1). Protein was expressed in *E. coli* BLR(DE3) grown in LB medium containing 100 µM IPTG and purified using the StrepTactin SpinPrep Kit (EMD Millipore). Protein purity was determined to be around 95% by SDS-PAGE and used directly for assay. In vitro reactions were carried out by combining 13.2 µg purified protein and 5 mM substrate in assay buffer (50 mM TrisCl (pH 7.5), 150 mM NaCl, 10 mM $MgCl_2$, 5 mM DTT) and incubating at 37°C for 30 min (18). Following addition of methanol (HPLC grade, Sigma-Aldrich) to 50% (vol/vol), samples were analyzed by liquid chromatography-mass spectrometry (LC-MS) alongside a DXP standard (Echelon Inc., Salt Lake City, Utah, USA). Chromatographic separation was achieved using an Agilent 1200 Rapid Resolution HPLC system using the hydrophilic interaction liquid chromatography (HILIC) method from Baidoo et al. (19) and metabolites were detected by an Agilent 6210 TOF MS system as described previously (20).

Terpene biosynthesis in *E. coli*. Amorphadiene production was compared using the original Δ*dxs*MB parent strain and an equivalent strain harboring a single mutation encoding RibB(G92D). Strains were transformed with the pADS plasmid, encoding amorphadiene synthase from *Artemisia annua* (15), and grown at 37°C in M9 medium (Sigma-Aldrich) containing 1% xylose, 0.5 mM IPTG, and a 10% (v/v) dodecane (Sigma-Aldrich) overlay (to capture amorphadiene), with or without 5 mM mevalonate. Amorphadiene production was measured by gas chromatography-mass spectrometry (GC-MS) as described previously (21).

Bisabolene production was tested in *E. coli* BL21(DE3) harboring a plasmid containing an nDXP gene, or *rfp* (encoding RFP, red fluorescent protein) as a control, and a second plasmid harboring the *Abies grandis* bisabolene synthase (AgBIS) gene, amplified from pRSLeu2d-BISopt (22), coupled with *E. coli* DXP pathway genes *ispD*, *ispF*, and *idi* (Fig. 1; see Table 1 for cloning details). The nDXP genes were expressed on pTrc99A plasmids as described above, while *AgBIS* and the DXP pathway genes were expressed on pBbA1k (23). Strains were grown at 37°C in EZ-X medium containing a 20% (v/v) dodecane overlay to an OD of around 1.0, at which point IPTG (200 µM) was added and growth was continued at 30°C; bisabolene was measured by GC-MS as described previously (22).

Vectors encoding translation fusions between Dxr (encoded by the *E. coli ispC* gene) and either RibB(G108S) or YajO, were constructed using the sequence and ligation-independent cloning (SLIC) approach (24). A combination of fusions was made with Dxr located either at the N- or C-terminus, and employing the peptide linkers G2 (GSGGSG), GP (GPGP), or PT (PTPTPTTPTPT) (Table 1). Fusions were expressed on pTrc99A plasmids while *AgBIS* combined with *E. coli* DXP pathway genes *ispD*, *ispF*, *idi*, and/or *ispA* were expressed on pBbA1k. Strains were grown in EZ-X medium and bisabolene quantified as described above.

Quantification of DXP pathway intermediates. DXP pathway intermediates were extracted from *E. coli* by brief centrifugation (3000 x g, 3 min, room temp) of each 5 mL culture, removal of medium, addition of 1 mL ice-cold 50% methanol (vol/vol in water) to the cell pellet, vortexing for one minute, centrifugation (15000 x g, 10 min, 4°C), and removal of high MW material from the supernatant by centrifugation (14,000 x g, 45 min, 4°C) through a 3000 MWCO Amicon Ultra 0.5 mL filter (Millipore, Carrigtwohill, Cork, Ireland). Separation of DXP

184 pathway intermediates and quantification using authentic standards (Echelon Inc.) was
185 performed using LC-MS as described above.
186
187 **RESULTS**
188 **Use of selective pressure to isolate spontaneous nDXP mutations.** The strain Δ*dxs*MB was
189 constructed to screen for nDXP routes by transforming *E. coli* MG1655 with the plasmid pMBI
190 and deletion of the *dxs* gene. pMBI, which encodes the lower half of the mevalonate pathway,
191 enables growth of Δ*dxs*MB in the presence of exogenously supplied mevalonate. A selection for
192 spontaneous nDXP mutants was carried out by subculturing in defined medium containing
193 xylose (EZ-X), coupled with reduction of the mevalonate concentration to growth-limiting
194 levels. Aliquots of each subculture were plated on EZ-X agar lacking mevalonate and colonies
195 were picked for further analysis. Since mutations in the native *aceE* gene have been reported to
196 complement a *dxs* knockout (25), the *aceE* gene was sequenced in the first 50 isolates but no
197 mutations were found.
198 **Sequencing of mevalonate-independent Δ*dxs*MB strains.** The genomes of eight strains
199 that were isolated at the beginning of the selection process were sequenced and all found to have
200 single nucleotide mutations in the *ribB* gene, encoding either S89R (three isolates), G92D (three
201 isolates), or T106I (two isolates). The wild type RibB enzyme is responsible for synthesis of the
202 riboflavin precursor 3,4-Dihydroxy-2-Butanone 4-Phosphate (DHBP) from Ru5P (13, 26).We
203 also sequenced the genomes of four strains isolated at the end of the screening process
204 (following three weeks of subculturing under selective pressure) and all three were found to
205 harbor mutations in *gatC* gene, encoding D296A. GatC functions as a galactitol
206 phosphotransferase permease and has also been found to contribute to xylose uptake (27, 28).

Since the strains harboring *ribB* mutations had grown considerably faster than those harboring *gatC* mutations on EZ-X agar lacking mevalonate (three versus six days, respectively), the RibB mutants were investigated further as the most promising nDXP candidates.

Generation of additional *ribB* mutants. Following chemical and EP-PCR mutagenesis of the *ribB* cds, mutant libraries were constructed in pTrc99A and transformed into Δ*dxs*MB. Selection in EZ-X was carried out as before and the 44 fastest-growing isolates were sequenced and found to comprise five discrete mutations: G108S, T88I, V109I, M182I, and G92D (see Table S1 in the supplemental material). 16 mutants that formed colonies within the first 24 hours were represented by two mutations, G108S and T88I. Complementation of Δ*dxs* by three of the *rib*B mutants was compared by expression on pTrc99A in Δ*dxs*MB, and culturing in the absence of mevalonate in either EZ-X or EZ-G (EZ-Rich medium containing 1% D-glucose) (Fig. 2). Expression of *ribB*(G108S) facilitated growth on either glucose or xylose in the absence of mevalonate at rates similar to those in media containing mevalonate. The growth rate of the *ribB*(G92D) strain was appreciably slower while negligible growth was observed in the strain containing an empty vector.

Rational selection of candidate nDXP genes. We selected candidate genes from several species on the basis of genetic or biochemical evidence of possible connections to both C5 sugars and DXP, and investigated their capacity to complement a *dxs* knockout. One of these genes, *yajO* from *E. coli*, was found to support growth on EZ-X agar in the absence of mevalonate when overexpressed in Δ*dxs*MB. Two lines of evidence had led to the selection of *yajO*, originally annotated to encode a putative xylose reductase, as a candidate nDXP gene. First, *yajO* was identified in a screen for genes linked to thiamine biosynthesis that employed growth-inhibiting thiamine analog precursors (29). Although the mechanism for resistance to

these analogs has not been elucidated, one of the possibilities is increased synthesis of DXP, a precursor to thiamine. Second, *yajO* together with the isoprenoid biosynthetic genes *dxs* and *ispA* (the latter encodes farnesyl pyrophosphate synthase) comprise an operon in the genomes of *E. coli* and related species.

Colony formation for Δ*dxs*MB harboring pTrc99A-*yajO* on EZ-X agar plates lacking mevalonate usually took 4-5 days. Efforts to make this route more efficient through mutagenesis of *yajO* followed by mevalonate selective pressure were unsuccessful. In addition, growth in defined media lacking mevalonate was observed when xylose but not glucose was provided as sole carbon source (see Fig. S1 in the supplemental material).

Reactions catalyzed by RibB(G108S) and YajO. To elucidate the reactions catalyzed by the nDXP enzymes, RibB(G108S) and YajO containing C-terminal StrepII tags were overexpressed in *E. coli* and purified. In vitro assays were conducted using candidate substrates xylose, xylulose, xylulose 5-phospate, and Ru5P, followed by analysis by LC-MS for potential products DXP and 1-deoxy-D-xylulose (DX). Production of DX was considered as a possible nDXP route, since DX can be phosphorylated to DXP by the endogenous *E. coli* xylulokinase, XylB (30). In the case of both enzymes DXP was detected only when Ru5P was included as substrate (Fig. 3). The addition of cofactors NADH, NADPH, or ATP to the reactions (at 1 mM) did not yield an increase in DXP and no product was detected when the wild type RibB enzyme was used instead of RibB(G108S) (data not shown).

Utility of nDXP routes for terpene production in *E. coli*. Initially the use of an nDXP route for isoprenoid production was evaluated by transforming Δ*dxs*MB harboring a genomic *ribB*(G92D) mutation and the corresponding parent strain with pADS, encoding amorphadiene synthase from *A. annua* (15). As expected, growth and amorphadiene production were negligible

253 in the parent strain in the absence of mevalonate while the corresponding *ribB*(G92D) strain
254 grew normally and generated 2 mg/L amorphadiene (see Fig. S2 in the supplemental material).
255 When supplemented with 5 mM mevalonate, strains grew to equivalent ODs, but the
256 amorphadiene titer (5.4 mg/L or 17 mg/g DCW) was over 4-fold higher in the *ribB*(G92D)
257 mutant compared to the control strain.

258 In order to evaluate the use of nDXP enzymes for terpene pathway engineering alongside
259 native levels of Dxs, the host strain was changed from Δ*dxs*MB to *E. coli* BL21(DE3). In
260 addition, we selected the candidate biofuel α-bisabolene as the target sesquiterpene product. To
261 assess synergy between DXP pathway engineering and nDXP routes, we constructed vectors for
262 expression of bisabolene synthase (AgBIS) together with DXP pathway enzymes that have
263 previously been shown to limit pathway flux, namely *ispD*, *ispF*, *idi*, and *ispA* (31). Expression
264 of *yajO* or *ribB*(G108S) alongside the plasmid pBbA1k-*AgBIS-ispDF-idi* yielded a 2-3 fold
265 improvement in bisabolene titers compared to an *rfp* control vector (Fig. 4A). Having previously
266 tested fusions of Dxs/Dxr for DXP pathway engineering and finding no benefit in terms of
267 bisabolene titer (data not shown), we constructed nDXP/Dxr fusions, using the native *ispC* gene
268 encoding Dxr, to determine if pathway flux could be enhanced. By comparison of several fusions
269 in which the order of proteins and the peptide linkers were varied, *ispC*-G2-*ribB*(G108S), where
270 G2 corresponds to a GSGGSG linker, yielded the highest increase in bisabolene titer (see Fig. S3
271 in the supplemental material).

272 To further investigate the *ispC*-G2-*ribB*(G108S) fusion, we first coupled it with three
273 different vectors harboring *AgBIS* and DXP pathway genes (Fig. 4B). The overall bisabolene
274 titer as well as the increase over control levels became progressively higher as the *ispC*-G2-
275 *ribB*(G108S) fusion was coupled with progressively engineered DXP pathway vectors. Coupling

pTrc99A-*ispC*-G2-*ribB*(G108S) with pBbA1k-*AgBIS-ispA-ispDF-idi* (Afii) yielded a 4.3-fold increase over controls levels in which Afii was coupled with *rfp*. To determine how this affects DXP pathway flux, we measured pathway intermediates in these two strains (Table 2). In the RFP control strain only two metabolites were detected, DXP and MEcPP (2-C-Methyl-D-erythritol 2,4-cyclophosphate), the latter being the substrate for IspG which is known to be kinetically slow (32). In the equivalent strain harboring pTrc99A-*ispC*-G2-*ribB*(G108S), DXP did not accumulate to detectable levels while MEcPP levels were almost 3-fold higher than the *rfp* strain. Together these data suggest that fusion of Dxr to RibB increases flux through the pathway, circumvents accumulation of DXP, and results in increased accumulation of MEcPP, implicating IspG as a suitable target for further engineering studies.

DISCUSSION

Metabolic engineering of terpene production in microbes or plants usually entails overexpression of key enzymes in the mevalonate or DXP precursor pathways (33). Dxs is an important control point in the DXP pathway as demonstrated by the fact that overexpression has increased terpene titers in several species (34, 35). However, the benefit gained by increasing Dxs levels is somewhat limited by regulatory mechanisms that can occur post-transcriptionally (36, 37), for example via feedback inhibition by prenyl phosphates (12, 38). The nDXP enzymes described here provide alternative routes to DXP that may facilitate terpene pathway engineering by circumventing regulatory issues and also carbon-loss associated with the Dxs-catalyzed reaction (Fig. 1). Additional benefits may arise depending on the carbon source provided to the production host; for example, nDXP expression may benefit *E. coli* grown on mixed sugars derived from hemicellulosic feedstocks by shunting the pentose fraction more directly to the

DXP pathway following conversion to Ru5P. Alternatively, engineering nDXP in plants and algae could provide a more direct link from carbon-fixation (Ru5P in the Calvin cycle) to the terpene pathway.

Calculation of the stoichiometric pathway efficiency, accounting for the cost of NADPH and ATP utilized together with the molar product yield (10), reveals that the nDXP route is more efficient not only from pentoses but also from glucose. Conversion of glucose 6-phosphate to Ru5P via the oxidative phase of the pentose phosphate pathway generates 2 NADPH, which may serve as cofactors in the DXP pathway. The resulting pathway efficiency of producing terpenes from glucose via the nDXP route is close to the maximum biochemical yield (0.309 grams bisabolene per gram of glucose versus 0.324 grams, respectively).

Our approach to screening for nDXP genes entailed growth on xylose as sole carbon source. Interestingly, mutations in the *aceE* gene, previously shown to convert pyruvate and glyceraldehyde to DX (25), were not encountered in any of the first 50 mevalonate prototrophs isolated, perhaps indicative that the mutant RibB route to DXP is more efficient than the mutant AceE route in the presence of high Ru5P levels. Overexpression of *ribB*(G108S) also enabled normal growth in the absence of mevalonate of Δ*dxs*MB on glucose, while overexpression of *yajO* enabled growth only on xylose, suggesting that YajO may require higher Ru5P levels to support growth due to kinetic limitations.

The remaining genomic mutation found to complement growth in Δ*dxs*MB, encoding GatC(D296A), was not investigated further. However, since GatC can function as an ATP-independent xylose transporter, it seems likely that the main benefit from the mutation may be increased uptake of xylose (27), perhaps increasing the Ru5P concentration to the point where native levels of YajO can generate sufficient DXP to sustain a low level of growth.

Two mutations in *ribB* have been recently found to complement Δ*dxs* in *E. coli* grown on LB medium (20); here we have identified one of the same mutations (G108S) along with 6 others (T88I, S89R, G92D, T106I, V109I, and M182I) that complement Δ*dxs* in *E. coli* grown on xylose and elucidated the reaction catalyzed. NMR and crystal structures have been solved for RibB from *E. coli* and other species, and a reaction mechanism has been proposed for conversion of Ru5P to the riboflavin precursor DHBP (39-42). Several of the RibB mutations that enable production of DXP are at or close to catalytically important residues; for example, G108 is conserved among RibB proteins from diverse sources and is suggested by NMR studies to play a role in substrate binding (40) while crystal structure analysis suggests a non-glycine residue at this critical turn would result in a sterically strained conformation (41). Since the reaction mechanism proposed for wt RibB involves the generation of 1-deoxy intermediates, one possibility is that the mutations result in termination of the reaction prior to the proposed carbon rearrangement and elimination of formate (26, 41). However, exact mechanism and means of reduction remains unknown and will require further investigation.

Although the reaction catalyzed by the mutant RibB enzyme is unusual, it is not completely unique; YajO from *E. coli* can also catalyze formation of DXP from Ru5P, albeit less efficiently. YajO was originally annotated as a putative xylose reductase, but little evidence was found for this activity in vitro and *E. coli* is known to utilize the alternative xylose isomerase route for xylose assimilation (14). YajO is now most often annotated as a 2-carboxybenzaldehyde reductase based on detection of this activity in vitro, but since *E. coli* is not known for polyaromatic hydrocarbon degradation, the true biological function for the enzyme remains unknown (14). It is tempting to speculate that YajO may play a role in biosynthesis of DXP (which, besides its role in the isoprenoid pathway, serves as a precursor to

345 thiamine) under conditions of thiamine starvation. Since Dxs requires thiamine pyrophosphate as
346 a cofactor, thiamine starvation would leave cells in a state where synthesis of DXP for de-novo
347 thiamine (and isoprenoid) biosynthesis would not be possible. YajO could serve a role in low
348 level DXP biosynthesis from Ru5P to kick-start thiamine biosynthesis and consequently Dxs. As
349 mentioned, *yajO* is located next to *dxs* on the *E. coli* genome and *ThiL*, which encodes the final
350 enzyme in the thiamine biosynthetic pathway, is situated less than 1 kb downstream.
351 Having demonstrated the utility of nDXP genes in engineering terpene production in *E.*
352 *coli*, we investigated the use of protein fusions to further increase yields of the candidate biofuel
353 bisabolene. The use of fusions or scaffolds has been demonstrated to increase pathway flux in
354 several situations, including terpene pathway engineering (43, 44). Having found that Dxs/Dxr
355 fusions (in either orientation, both using GSGGSG linkers) did not yield an increase in
356 bisabolene titer we tested Dxr/nDXP fusions, where nDXP was either *yajO* or *ribB*(G108S), and
357 found that *ispC*-G2-*ribB*(G108S) yielded a 4.3 improvement in bisabolene production over the
358 control strain. The fact that DXP accumulation was below the limit of detection in this strain
359 suggests that metabolic flux from Ru5P to MEP is efficient. However, extensive further
360 engineering of the DXP pathway will be required to achieve terpene yields close the theoretical
361 maximum in *E. coli*. Our analysis of DXP pathway intermediates, together with previously
362 published studies, suggest that IspG is a key pathway bottleneck that should be addressed
363 together with the genes expressed here (45, 46).We are also currently investigating the utility of
364 the nDXP genes and fusions in plant hosts where a direct link from carbon fixation to biofuel
365 production presents an attractive opportunity.
366
367 ACKNOWLEDGEMENTS

J.D.K. has a financial interest in Amyris and Lygos.

The work conducted through the Joint BioEnergy Institute was supported by the Office of Science, Office of Biological and Environmental Research, of the U.S. Department of Energy under Contract No. DE-AC02-05CH11231. The work conducted through the University of California at Berkeley was funded through the U.S. Dept. of Energy ARPA-E PETRO program, under grant No. DE-AR0000209.

1. Perez-Gil J, Rodriguez-Concepcion M. 2013. Metabolic plasticity for isoprenoid biosynthesis in bacteria. The Biochemical journal 452:19-25.

2. Tippmann S, Chen Y, Siewers V, Nielsen J. 2013. From flavors and pharmaceuticals to advanced biofuels: production of isoprenoids in Saccharomyces cerevisiae. Biotechnology journal 8:1435-1444.

3. Boucher Y, Doolittle WF. 2000. The role of lateral gene transfer in the evolution of isoprenoid biosynthesis pathways. Molecular microbiology 37:703-716.

4. Skjanes K, Rebours C, Lindblad P. 2013. Potential for green microalgae to produce hydrogen, pharmaceuticals and other high value products in a combined process. Critical reviews in biotechnology 33:172-215.

5. Ye VM, Bhatia SK. 2012. Pathway engineering strategies for production of beneficial carotenoids in microbial hosts. Biotechnology letters 34:1405-1414.

6. Onrubia M, Cusido RM, Ramirez K, Hernandez-Vazquez L, Moyano E, Bonfill M, Palazon J. 2013. Bioprocessing of plant in vitro systems for the mass production of pharmaceutically important metabolites: paclitaxel and its derivatives. Current medicinal chemistry 20:880-891.

7. Paddon CJ, Westfall PJ, Pitera DJ, Benjamin K, Fisher K, McPhee D, Leavell MD, Tai A, Main A, Eng D, Polichuk DR, Teoh KH, Reed DW, Treynor T, Lenihan J, Fleck M, Bajad S, Dang G, Dengrove D, Diola D, Dorin G, Ellens KW, Fickes S, Galazzo J, Gaucher SP, Geistlinger T, Henry R, Hepp M, Horning T, Iqbal T, Jiang H, Kizer L, Lieu B, Melis D, Moss N, Regentin R, Secrest S, Tsuruta H, Vazquez R, Westblade LF, Xu L, Yu M, Zhang Y, Zhao L, Lievense J, Covello PS, Keasling JD, Reiling KK, Renninger NS, Newman JD. 2013. High-level semi-synthetic production of the potent antimalarial artemisinin. Nature 496:528-532.

8. Du J, Shao Z, Zhao H. 2011. Engineering microbial factories for synthesis of value-added products. Journal of industrial microbiology & biotechnology 38:873-890.

9. Li H, Cann AF, Liao JC. 2010. Biofuels: biomolecular engineering fundamentals and advances. Annual review of chemical and biomolecular engineering 1:19-36.

10. Dugar D, Stephanopoulos G. 2011. Relative potential of biosynthetic pathways for biofuels and bio-based products. Nature biotechnology 29:1074-1078.

11. Scheller HV, Ulvskov P. 2010. Hemicelluloses. Annual review of plant biology 61:263-289.

12. **Banerjee A, Wu Y, Banerjee R, Li Y, Yan H, Sharkey TD. 2013. Feedback inhibition of deoxy-D-xylulose-5-phosphate synthase regulates the methylerythritol 4-phosphate pathway. The Journal of biological chemistry 288:16926-16936.**
13. **Richter G, Volk R, Krieger C, Lahm HW, Rothlisberger U, Bacher A. 1992. Biosynthesis of riboflavin: cloning, sequencing, and expression of the gene coding for 3,4-dihydroxy-2-butanone 4-phosphate synthase of Escherichia coli. Journal of bacteriology 174:4050-4056.**
14. **Ko J, Kim I, Yoo S, Min B, Kim K, Park C. 2005. Conversion of methylglyoxal to acetol by Escherichia coli aldo-keto reductases. Journal of bacteriology 187:5782-5789.**
15. **Martin VJ, Pitera DJ, Withers ST, Newman JD, Keasling JD. 2003. Engineering a mevalonate pathway in Escherichia coli for production of terpenoids. Nature biotechnology 21:796-802.**
16. **Datsenko KA, Wanner BL. 2000. One-step inactivation of chromosomal genes in Escherichia coli K-12 using PCR products. Proceedings of the National Academy of Sciences of the United States of America 97:6640-6645.**
17. **Rose MD, Fink GR. 1987. KAR1, a gene required for function of both intranuclear and extranuclear microtubules in yeast. Cell 48:1047-1060.**
18. **Schlosser T, Schmidt G, Stahmann KP. 2001. Transcriptional regulation of 3,4-dihydroxy-2-butanone 4-phosphate synthase. Microbiology 147:3377-3386.**
19. **Baidoo EE, Xiao Y, Dehesh K, Keasling JD. 2014. Metabolite profiling of plastidial deoxyxylulose-5-phosphate pathway intermediates by liquid chromatography and mass spectrometry. Methods Mol Biol 1153:57-76.**
20. **Perez-Gil J, Uros EM, Sauret-Gueto S, Lois LM, Kirby J, Nishimoto M, Baidoo EE, Keasling JD, Boronat A, Rodriguez-Concepcion M. 2012. Mutations in Escherichia coli aceE and ribB genes allow survival of strains defective in the first step of the isoprenoid biosynthesis pathway. PloS one 7:e43775.**
21. **Paradise EM, Kirby J, Chan R, Keasling JD. 2008. Redirection of flux through the FPP branch-point in Saccharomyces cerevisiae by down-regulating squalene synthase. Biotechnology and bioengineering 100:371-378.**
22. **Peralta-Yahya PP, Ouellet M, Chan R, Mukhopadhyay A, Keasling JD, Lee TS. 2011. Identification and microbial production of a terpene-based advanced biofuel. Nature communications 2:483.**
23. **Lee TS, Krupa RA, Zhang F, Hajimorad M, Holtz WJ, Prasad N, Lee SK, Keasling JD. 2011. BglBrick vectors and datasheets: A synthetic biology platform for gene expression. Journal of biological engineering 5:12.**
24. **Li MZ, Elledge SJ. 2007. Harnessing homologous recombination in vitro to generate recombinant DNA via SLIC. Nature methods 4:251-256.**
25. **Sauret-Gueto S, Uros EM, Ibanez E, Boronat A, Rodriguez-Concepcion M. 2006. A mutant pyruvate dehydrogenase E1 subunit allows survival of Escherichia coli strains defective in 1-deoxy-D-xylulose 5-phosphate synthase. FEBS letters 580:736-740.**
26. **Bacher A, Eberhardt S, Fischer M, Kis K, Richter G. 2000. Biosynthesis of vitamin b2 (riboflavin). Annual review of nutrition 20:153-167.**
27. **Nduko JM, Matsumoto K, Ooi T, Taguchi S. 2014. Enhanced production of poly(lactate-co-3-hydroxybutyrate) from xylose in engineered Escherichia coli**

overexpressing a galactitol transporter. Applied microbiology and biotechnology 98:2453-2460.

28. Nobelmann B, Lengeler JW. 1996. Molecular analysis of the gat genes from Escherichia coli and of their roles in galactitol transport and metabolism. Journal of bacteriology 178:6790-6795.

29. Lawhorn BG, Gerdes SY, Begley TP. 2004. A genetic screen for the identification of thiamin metabolic genes. The Journal of biological chemistry 279:43555-43559.

30. Hecht S, Eisenreich W, Adam P, Amslinger S, Kis K, Bacher A, Arigoni D, Rohdich F. 2001. Studies on the nonmevalonate pathway to terpenes: the role of the GcpE (IspG) protein. Proceedings of the National Academy of Sciences of the United States of America 98:14837-14842.

31. Yuan LZ, Rouviere PE, Larossa RA, Suh W. 2006. Chromosomal promoter replacement of the isoprenoid pathway for enhancing carotenoid production in E. coli. Metabolic engineering 8:79-90.

32. Xu W, Lees NS, Adedeji D, Wiesner J, Jomaa H, Hoffman BM, Duin EC. 2010. Paramagnetic intermediates of (E)-4-hydroxy-3-methylbut-2-enyl diphosphate synthase (GcpE/IspG) under steady-state and pre-steady-state conditions. Journal of the American Chemical Society 132:14509-14520.

33. Vickers CE, Bongers M, Liu Q, Delatte T, Bouwmeester H. 2014. Metabolic engineering of volatile isoprenoids in plants and microbes. Plant, cell & environment 37:1753-1775.

34. Kim SW, Keasling JD. 2001. Metabolic engineering of the nonmevalonate isopentenyl diphosphate synthesis pathway in Escherichia coli enhances lycopene production. Biotechnology and bioengineering 72:408-415.

35. Munoz-Bertomeu J, Arrillaga I, Ros R, Segura J. 2006. Up-regulation of 1-deoxy-D-xylulose-5-phosphate synthase enhances production of essential oils in transgenic spike lavender. Plant physiology 142:890-900.

36. Cordoba E, Salmi M, Leon P. 2009. Unravelling the regulatory mechanisms that modulate the MEP pathway in higher plants. Journal of experimental botany 60:2933-2943.

37. Wright LP, Rohwer JM, Ghirardo A, Hammerbacher A, Ortiz-Alcaide M, Raguschke B, Schnitzler JP, Gershenzon J, Phillips MA. 2014. Deoxyxylulose 5-Phosphate Synthase Controls Flux through the Methylerythritol 4-Phosphate Pathway in Arabidopsis. Plant physiology 165:1488-1504.

38. Ghirardo A, Wright LP, Bi Z, Rosenkranz M, Pulido P, Rodriguez-Concepcion M, Niinemets U, Bruggemann N, Gershenzon J, Schnitzler JP. 2014. Metabolic flux analysis of plastidic isoprenoid biosynthesis in poplar leaves emitting and nonemitting isoprene. Plant physiology 165:37-51.

39. Steinbacher S, Schiffmann S, Richter G, Huber R, Bacher A, Fischer M. 2003. Structure of 3,4-dihydroxy-2-butanone 4-phosphate synthase from Methanococcus jannaschii in complex with divalent metal ions and the substrate ribulose 5-phosphate: implications for the catalytic mechanism. The Journal of biological chemistry 278:42256-42265.

40. Kelly MJ, Ball LJ, Krieger C, Yu Y, Fischer M, Schiffmann S, Schmieder P, Kuhne R, Bermel W, Bacher A, Richter G, Oschkinat H. 2001. The NMR structure of the 47-kDa dimeric enzyme 3,4-dihydroxy-2-butanone-4-phosphate synthase and ligand

binding studies reveal the location of the active site. Proceedings of the National Academy of Sciences of the United States of America 98:13025-13030.

41. Liao DI, Calabrese JC, Wawrzak Z, Viitanen PV, Jordan DB. 2001. Crystal structure of 3,4-dihydroxy-2-butanone 4-phosphate synthase of riboflavin biosynthesis. Structure 9:11-18.

42. Volk R, Bacher A. 1991. Biosynthesis of riboflavin. Studies on the mechanism of L-3,4-dihydroxy-2-butanone 4-phosphate synthase. The Journal of biological chemistry 266:20610-20618.

43. Dueber JE, Wu GC, Malmirchegini GR, Moon TS, Petzold CJ, Ullal AV, Prather KL, Keasling JD. 2009. Synthetic protein scaffolds provide modular control over metabolic flux. Nature biotechnology 27:753-759.

44. Brodelius M, Lundgren A, Mercke P, Brodelius PE. 2002. Fusion of farnesyldiphosphate synthase and epi-aristolochene synthase, a sesquiterpene cyclase involved in capsidiol biosynthesis in Nicotiana tabacum. European journal of biochemistry / FEBS 269:3570-3577.

45. Rivasseau C, Seemann M, Boisson AM, Streb P, Gout E, Douce R, Rohmer M, Bligny R. 2009. Accumulation of 2-C-methyl-D-erythritol 2,4-cyclodiphosphate in illuminated plant leaves at supraoptimal temperatures reveals a bottleneck of the prokaryotic methylerythritol 4-phosphate pathway of isoprenoid biosynthesis. Plant, cell & environment 32:82-92.

46. Zhou K, Zou R, Stephanopoulos G, Too HP. 2012. Metabolite profiling identified methylerythritol cyclodiphosphate efflux as a limiting step in microbial isoprenoid production. PloS one 7:e47513.

Table 1 Primers used in this study

Target gene	Primer name	Primer sequence
[a]*Dxs* knockout	Dxs-KO-f	atgagttttgatattgccaaataccgaccctggcactggtcgactccacgtgtaggctggagctgcttcg
	Dxs-KO-r	ttctacggtgaccagcgcttcatggctggcggccatttccagaattaacgatgggaattagccatggtcc
ribB	pTrc-ribB-f	gaccatggcaaatcagacgctactttcctcttttggtacg (restriction site underlined)
	pTrc-ribB-r	ccaagctttcagctggctttacgctcatgtgcgtgac
[b]*yajO*	pTrc-yajO-f	aaccatggaacaatacaaccccttaggaaaaacc
	pTrc-yajO-r	aaaagctttttatttaaatcctacgacaggatgcg
ribB	pTrc-ribB-S-f	gaccatggcaaatcagacgctactttcc
(*StrepII tag*)	pTrc-ribB-S-r	ttaagctttca*tttttcaaactgcggatggctcca*gctggctttacgctcatgtgcc
yajO	pTrc-yajO-S-f	acatcgatgcaatacaaccccttagga
(*StrepII tag*)	pTrc-yajO-S-r	ttaagctttta*tttttcaaactgcggatggctcca*tttaaatcctacgacaggatgcg
AgBIS	pBbA1k-BIS-f	aagaattcagtttttccctactagttcaggaggtattcatggcgggtgtttctgcggtttctaaagtttcttctctgg
	pBbA1k-BIS-r	ttggatcctacagcggcagcggttcgatcaggca
[c]*ispA*	pBbA1k-ispA-f	aaggatcctctagaggaggtacactatggactttccgcagcaactcgaagc
	pBbA1k-ispA-r	aactcgagttatttattacgctggatgatgtag
[d]*ispDF*	pBbA1k-ispDF-f	cgctgccgctgtaaggatcccccgggaattaacatggcaa
	pBbA1k-ispDF-r	cataatttctcacatgtaattcattttgttgccttaatgagtagc
[d]*idi*	pBbA1k-idi-f	tcattaaggcaacaaaatgaattacatgtgagaaattatgc

	pBbA1k-idi-f	cctggagatccttactcgagttatttaagctgggtaaatg
[e]*yajO-ispC*	Ptrc-yajO-F-f	gaattgtgagcggataacaatttcacacaggaaacagaccatgactggggtgaacgaatgcag
	ispC-GP-f	aaaccgcatcctgtcgtaggatttaaa**ggtccaggccc**taagcaactcaccattctgggct
	yajO-GP-r	cggtcgagcccagaatgfgtgagttgctt**agggcctggacc**tttaaatcctacgacaggatgcggttt
	ispC-PT-f	cctgtcgtaggatttaaa**ccaacaccaacgccaacgacaccaactccaaca**aagcaactcaccattctgggc
	yajO-PT-r	agaatggtgagttgctt**tgttggagttggtgtcgttggcgttggtgttgg**tttaaatcctacgacaggatgcggtt
	ispC-Ptrc-r	ggctgaaaatcttctctcatccgccaaaacagccaagctttcagcttgcgagacgcatcac
[e]*ribB-ispC*	Ptrc-ribB-F-f	gaattgtgagcggataacaatttcacacaggaaacagaccatggcaaatcagacgctactttcctctttt
	IspC-G2-F-f	cgtcaggcacatgagcgtaaagccagc**ggttctggcggttccggt**aagcaactcaccattctgggct
	ribB-G2-r	gagccggtcgagcccagaatggtgagttgctt**accggaaccgccagaacc**gctggctttacgctcatgtgcctg
	ispC-GP-F-f	ccgtcaggcacatgagcgtaaagccagc**ggtccaggccct**aagcaactcaccattctgggctcg
	ribB-GP-r	gagccggtcgagcccagaatggtgagttgctt**agggcctggacc**gctggctttacgctcatgtgcctga
	ispC-Ptrc-r	ggctgaaaatcttctctcatccgccaaaacagccaagctttcagcttgcgagacgcatcac
[e]*ispC-yajO*	ispC-Ptrc-f	gaattgtgagcggataacaatttcacacaggaaacagaccatgaagcaactcaccattctgggct
	IspC-G2-r	ggctgcattcgttcaccccagt**accggaaccgccagaacc**gcttgcgagacgcatcacctctttt
	yajO-G2-f	aggtgatgcgtctcgcaagc**ggttctggcggttccggt**actggggtgaacgaatgcagc
	yajO-Ptrc-r	ggctgaaaatcttctctcatccgccaaaacagccaagcttttatttaaatcctacgacaggatgcggtttatacg
[e]*ispC-ribB*	IspC-Ptrc-f	gaattgtgagcggataacaatttcacacaggaaacagaccatgaagcaactcaccattctgggct
	IspC-G2-R-r	aaaagaggaaagtagcgtctgatttgc**accggaaccgccagaacc**gcttgcgagacgcatcacctc
	ribB-G2-f	tgatgcgtctcgcaagc**ggttctggcggttccggt**gcaaatcagacgctactttcctcttttgg
	ribB-Ptrc-r	ggctgaaaatcttctctcatccgccaaaacagccaagctttcagctggctttacgctcatgtgc

[a] The 50 nt at the 5' end of these primers matches the ends of the *dxs* cds while the underlined sequence matches the kanamycin resistance cassette. The kanamycin marker cassette was amplified by PCR from plasmid pDK13 (16) using the primers listed. *E. coli* MG1655 harboring pMBI was transformed with this PCR product together with the plasmid pKD46, containing the gene for γ Red recombinase (16). Following selection on LB-kanamycin, deletion of *dxs* was confirmed by several diagnostic PCRs, and loss of the temperature-sensitive pDK46 plasmid was facilitated by growth at 37°C.

[b] The *yajO* cds was selected according to the Genbank annotation for *E. coli* MG1655, beginning with the amino acid sequence MQYN. However, the *yajO* sequence in *E. coli* H736 is annotated to contain an additional 14 N-terminal amino acids (beginning MTGV) and the corresponding region in MG1655 forms a contiguous orf, but with a putative valine start codon (reading VTGV). Since it is uncertain whether translation of the MG1655 *yajO* cds begins at the annotated Met, or the Val codon 14 amino acids upstream, we overexpressed both versions in Δ*dxs*MB (but substituting Met for Val in the longer version) and found that they both complemented the *dxs* knockout.

[c] The *ispA* cds (encoding FPP synthase) was amplified from *E. coli* MG1655 genomic DNA and cloned between the BamHI and XhoI sites of pBbA1k-AgBIS to make the plasmid pBbA1k-AgBIS-*ispA* (pBbA1k-AF).

[d] The *ispDF* operon and *idi* gene were amplified from *E. coli* MG1655 genomic DNA and cloned between the BamHI and XhoI sites of pBbA1k-AgBIS using SLIC to make the plasmid pBbA1k-AgBIS-*ispDF-idi* (pBbA1k-Aii). Sequences homologous to each other or to the vector backbone

are underlined. This fragment was subsequently cloned into the XhoI site of pBbA1k-AgBIS-*ispA* to make the plasmid pBbA1k-AgBIS-*ispA*- *ispDF-idi* (pBbA1k-AFii).

[e] nDXP-Dxr fusions were constructed by PCR SOEing (Splicing by Overlap Extension). Three fusions each for yajO/ispC and ribB/ispC were constructed and cloned between the NcoI and HindIII sites of pTrc99A. Nucleotides encoding fusion linkers (GP, GPGP; PT, PTPTPTTPTPT; G2, GSGGSG) are shown in bold.

TABLE 2 Measurement of DXP pathway intermediates in two *E. coli* strains engineered for bisabolene production. Vectors harboring *rfp* or an *ispC*-G2-*ribB*(G108S) fusion (Dxr-RibB) were coupled with pBbA1k-*AgBIS-ispA-ispDF-idi* (Afii). Concentrations are in µM and normalized to culture OD; standard deviations from three cultures are shown in parentheses.

	DXP	MEP	CDP-ME	MEcPP	HDMAPP	IPP/DMAPP
Afii + RFP	1.13 (0.62)	0.00	0.00	13.9 (5.2)	0.00	0.00
Afii + Dxr-RibB	0.00	0.15 (0.01)	0.43 (0.06)	38.7 (13.3)	0.00	0.00

FIGURE LEGENDS

FIG 1 The DXP pathway, together with the alternative nDXP route from Ru5P. IPP, isopentenyl pyrophosphate; DMAPP, dimethylallyl pyrophosphate.

FIG 2 Growth of *E. coli* Δ*dxs*MB expressing various *ribB* mutants on pTrc99A on glucose or xylose as sole carbon source. Supplementation of the RibB(G108S) strain with 1 mM mevalonate makes no significant difference to growth rate. The Δ*dxs*MB strain harboring an empty vector exhibited minimal growth within 24 hours.

575

576 **FIG 3** In vitro production of DXP (5.7 min) from Ru5P by RibB(G108S) and YajO. (A) to (D)
577 Chromatograms for DXP produced in vivo by yajO (A) and RibB(G108S) (C), and the same
578 samples spiked with 4 µM DXP to confirm the retention time for DXP, (B) and (D) respectively.
579 Mass spectra for a DXP standard (E) and DXP produced by RibB(G108S) (F).

580

581 **FIG 4** Bisabolene production via the DXP pathway in *E. coli* using nDXP genes. (A) Expression
582 of *rfp*, *yajO*, or *ribB(G108S*) combined with pBbA1k-*AgBIS*-i*spDF*-*idi*. (B) Expression of *rfp* or
583 an *ispC*-*(GSG)*$_2$-*ribB(G108S)* fusion (ispC-ribB) coupled with either pBbA1k-*AgBIS*-*ispA* (AF),
584 pBbA1k-*AgBIS*-*ispDF*-*idi* (Aii), or pBbA1k-*AgBIS*-*ispA*-*ispDF*-*idi* (Afii).

585

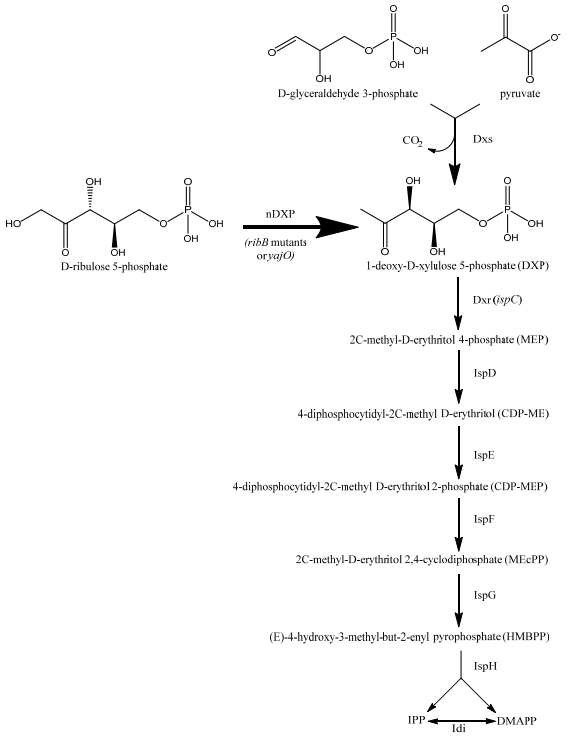

FIG 1 The DXP pathway, together with the alternative nDXP route from Ru5P. IPP, isopentenyl pyrophosphate; DMAPP, dimethylallyl pyrophosphate.

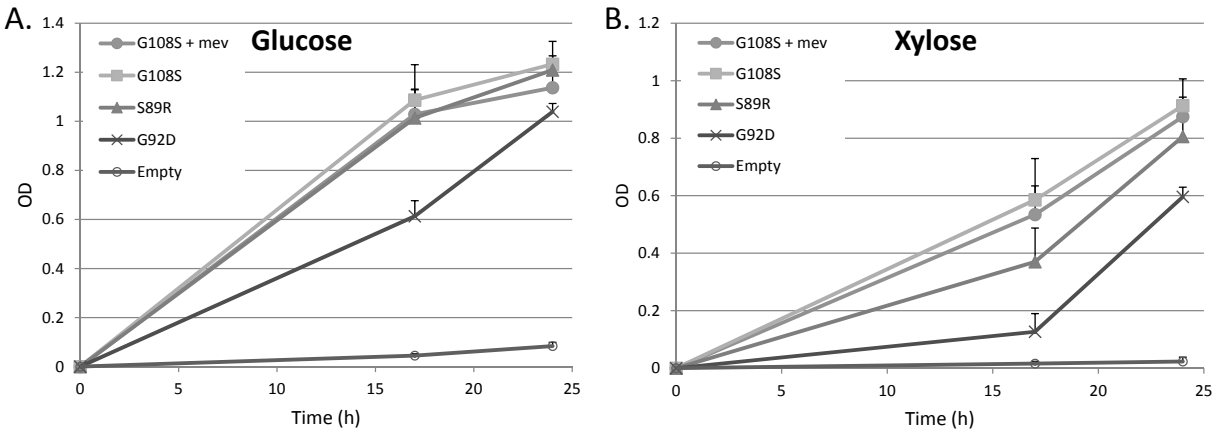

FIG 2 Growth of *E. coli* Δ*dxs*MB expressing various *ribB* mutants on pTrc99A on glucose or xylose as sole carbon source. Supplementation of the RibB(G108S) strain with 1 mM mevalonate makes no significant difference to growth rate. The Δ*dxs*MB strain harboring an empty vector exhibited minimal growth within 24 hours.

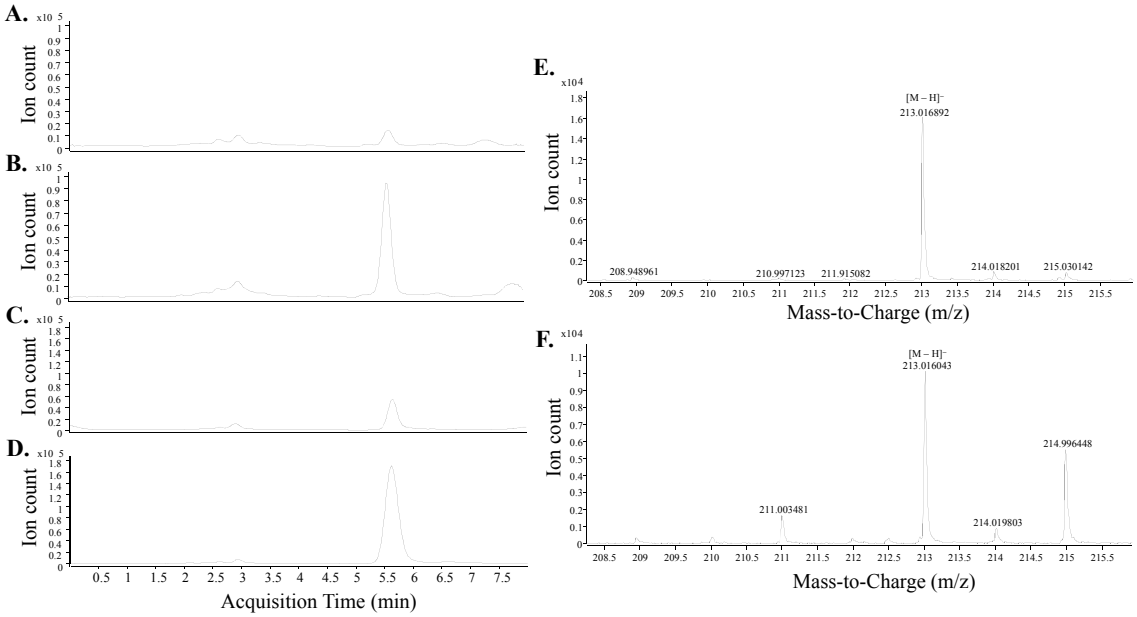

FIG 3 In vitro production of DXP (5.7 min) from Ru5P by RibB(G108S) and YajO. (A) to (D) Chromatograms for DXP produced in vitro by yajO (A) and RibB(G108S) (C), and the same samples spiked with 4 µM DXP to confirm the retention time for DXP, (B) and (D) respectively. Mass spectra for a DXP standard (E) and DXP produced by RibB(G108S) (F).

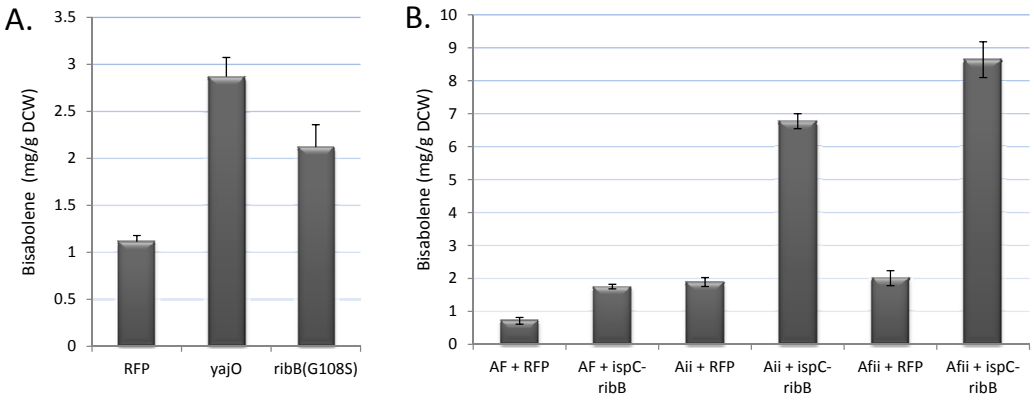

FIG 4 Bisabolene production via the DXP pathway in *E. coli* using nDXP genes. (A) Expression of *rfp*, *yajO*, or *ribB(G108S*) combined with pBbA1k-*AgBIS*-i*spDF-idi*. (B) Expression of *rfp* or an *ispC-(GSG)*$_2$*-ribB(G108S)* fusion (ispC-ribB) coupled with either pBbA1k-*AgBIS-ispA* (AF), pBbA1k-*AgBIS-ispDF-idi* (Aii), or pBbA1k-*AgBIS-ispA-ispDF-idi* (Afii).